Therefore,

$$P^* = 1 + \frac{P_{-\infty}}{P_{+\infty}} \gamma M_{-\infty}{}^2 \left(\sin\theta_0 + \frac{\gamma + 1}{4} \cos\theta_0 \cdot \Delta_0\right) \frac{d\eta}{d\xi} + \frac{P_{-\infty}}{P_{+\infty}} \gamma M_{-\infty}{}^2 \cos\theta_0 \cdot \frac{\gamma + 1}{4} \left(\frac{d\eta}{d\xi}\right)^2$$

$$= 1 + B\left(\frac{d\eta}{d\xi}\right) + C\left(\frac{d\eta}{d\xi}\right)^2 \quad (9)$$

where

$$B = (P_{-\infty}/P_{+\infty})\gamma M_{-\infty}{}^2(\sin\theta_0 + [(\gamma + 1)/4] \cos\theta_0 \cdot \Delta_0) \quad (10a)$$

and

$$C = (P_{-\infty}/P_{+\infty})\gamma M_{-\infty}{}^2 \cos\theta_0 \cdot [(\gamma + 1)/4] \quad (10b)$$

B. Special case of flat plate placed along direction of freestream

Here

$$\alpha = \theta_0 = \sin^{-1}1/M_{-\infty} = \sin^{-1}1/M_1$$

$$\cos\theta_0 \approx 1$$

for which $P_{+\infty}/P_{-\infty} = 1$ and $\Delta_0 = 0$. Equation (6b) becomes

$$P^* = 1 + \gamma M_1{}^2(1/M_1)\Delta_1 + \gamma M_1{}^2\theta_1\Delta_1$$

$$= 1 + \gamma M_1\Delta_1 + \gamma M_1{}^2\theta_1\Delta_1 \quad (11)$$

From Ref. 1, for the strong interaction case,

$$\theta_1 \approx [(\gamma + 1)/2]\Delta_1 \quad (12)$$

and, for weak interaction case,

$$\theta_1 \approx [(\gamma + 1)/4]\Delta_1 \quad (13)$$

Corresponding to (12), P^* is given from (11) as

$$P^* = 1 + \gamma M_1 \frac{d\eta}{d\xi} + \gamma M_1{}^2 \cdot \frac{(\gamma + 1)}{2} \left(\frac{d\eta}{d\xi}\right)^2 \quad \left(\text{since } \Delta_1 \approx \frac{d\eta}{d\xi}\right)$$

$$= 1 + \gamma k + \gamma \frac{(\gamma + 1)}{2} k^2 \quad (14)$$

where k is hypersonic similarily parameter $k = M_1(d\eta/d\xi)$. For (13), P^* is

$$P^* = 1 + \gamma k + \gamma[(\gamma + 1)/4]k^2 \quad (15)$$

Conclusion

In (14), i.e., for strong interaction case, if $(1 + \gamma k)$ is neglected in comparison to $[\gamma(\gamma + 1)/2]k^2$, since for this case $k \gg 2$, P^* becomes

$$P^* \approx [\gamma(\gamma + 1)/2]k^2$$

which is exactly the distribution represented by the tangent wedge.

Equation (15) contains the first three terms of the series for P^*, given by tne tangent wedge for the weak interaction case. Also when for weak interaction $P^* = 1 + \gamma k$ and for strong interaction $P^* \approx [\gamma(\gamma + 1)/2]k^2$, the pressure distribution for the whole flow system is often represented by $1 + \gamma k + \gamma[(\gamma + 1)/2]k^2$.

From (14) and (15), the forementioned case easily is seen to be

$$P^* = 1 + \gamma k + [\gamma(\gamma + 1)/4]k^2 + [\gamma(\gamma + 1)/2]k^2$$

If $[\gamma(\gamma + 1)/4]k^2$ is neglected, since for weak interaction case $k \ll 2$,

$$P^* = 1 + \gamma k + [\gamma(\gamma + 1)/2]k^2$$

which is the required distribution.

From the forementioned relations of (14) and (15), it is easy to see that the pressure distribution (6b) is in excellent agreement with the tangent-wedge approximation.

Reference

[1] Pai, S., "Hypersonic viscous flow over an insulated wedge at an angle of attack," Univ. Md. Rept. B.N. 42, Air Res. Dev. Command, Office Sci. Res. Rept. OSR-TN-54-321 (October 1954).

Capture of a Passively Stabilized Satellite by Earth's Gravity Field

D. H. DICKSTEIN*
General Electric Company, Philadelphia, Pa.

INTEREST is currently high in passive stabilization of spacecraft, particularly satellites of the earth. Of the several techniques of passive stabilization, use of earth's gravity field is receiving perhaps most attention. In this technique, the satellite's configuration is so arranged that torques are produced on the satellite by the gradient of earth's gravity field, restoring the satellite toward one of its equilibrium positions if displaced from equilibrium. Under the action of these torques, the satellite librates or oscillates about one of the equilibrium positions. If the satellite also contains some damping mechanism, the oscillations will decay until they fall within a small steady-state deadband about one of the equilibrium positions. The satellite is so configured that in its equilibrium position an antenna, for instance, is directed to earth.

The classic configuration that is torqued by earth's gravity gradient is a dumbbell. The dumbbell is oriented in pitch and roll but not yaw, where the yaw axis is the local vertical. Another configuration, one now being widely studied and developed, consists of a central body from which long thin-walled tubes uncoil once the satellite is in orbit. Because of their great length (hundreds of feet for some applications), the tubes endow the satellite with the necessary inertia to develop from the gravity field high restoring torques. If the tubes extend from the central body to form a cross having its two members at right angles and of unequal length, restoring torques in yaw, as well as pitch and roll, are developed. Yaw restoring torques are also developed if the rods extend to form an X, that is, with two members of equal length intersecting at an angle different from 90°.

A typical mission profile of such a gravity oriented satellite consists of the following:

1) Injection into orbit from a final propulsion stage either spin-stabilized such as Scout or containing its own attitude stabilization such as Agena. In the former instance the satellite, after separation from the propulsion stage, is itself spinning. In the latter instance the satellite is slowly tumbling after separation.

2) Conversion of the spinning or tumbling of the satellite to oscillation about the local vertical. Oscillation about the local vertical, when seen from inertial space, is a steady rotation of the satellite plus a superimposed oscillation. The rotation is about an axis normal to the orbital plane. The rotation is at a rate eoual to the satellite's orbital rate, which is much slower than the rate at injection. As seen from inertial space, then, the spinning or random tumbling at injection must be converted to a much slower rotation about an axis having a particular direction in space.

3) Decay of the satellite's oscillation. The oscillation decays to a small deadband whose width is determined by the

---

Received May 16, 1963; revision received August 2, 1963.

* Systems Project Engineer, Spacecraft Department. Member AIAA.

strength and frequency of the various cyclic disturbances acting on the satellite. Solar pressure on the tubes is an example of a cyclic disturbance, one having a period equal to orbital period.

Treated here is the second phase, the conversion of spinning or random tumbling to oscillation about the local vertical. This is called "capture" of the satellite by the earth.

The first phase of the mission profile involves the final propulsion stage and the separation mechanism.

The third phase of the mission profile involves the technique and mechanism by which oscillations of the satellite decay. Decay of oscillations involves two or more portions of the satellite coupled together with a damper and possibly also a spring. The capture phenomenon studied here involves only one rigid body acted on by gravity gradient torques. Under certain conditions of injection into orbit, the satellite captures without aid from the damper, whereas under other conditions, damping is necessary for capture. The conditions when damping is necessary for capture are not investigated; there are several techniques for damping, and each requires an elaborate analysis.

Tube Extension Rate

A satellite configuration having long tubes that uncoil and extend from a central body is chosen as a typical model. Practically, the tube extension mechanism gives extension rates of several tens of feet per minute. During extension, the tumbling satellite slows by conservation of angular momentum.

The basic condition for capture of a rigid body in a gravitational field is best seen in the limiting case of instantaneous tube extension. After the tubes have been extended, the satellite will be captured if its rate and position fall within the bounds shown in Fig. 1. These figures consider pitch, roll, and yaw separately; that is, the motion is planar. The figures show conditions of no capature when angular position of the tubes is aligned with the local vertical. However, by simply allowing the satellite to make several revolutions while the tubes are extending, these singular conditions are eliminated. Figure 2 shows the result of this "averaging out" process when the tubes are extended in half an hour. For other tube extension periods during which the satellite makes at least several revolutions, the capture maps would be similar to Fig. 2.

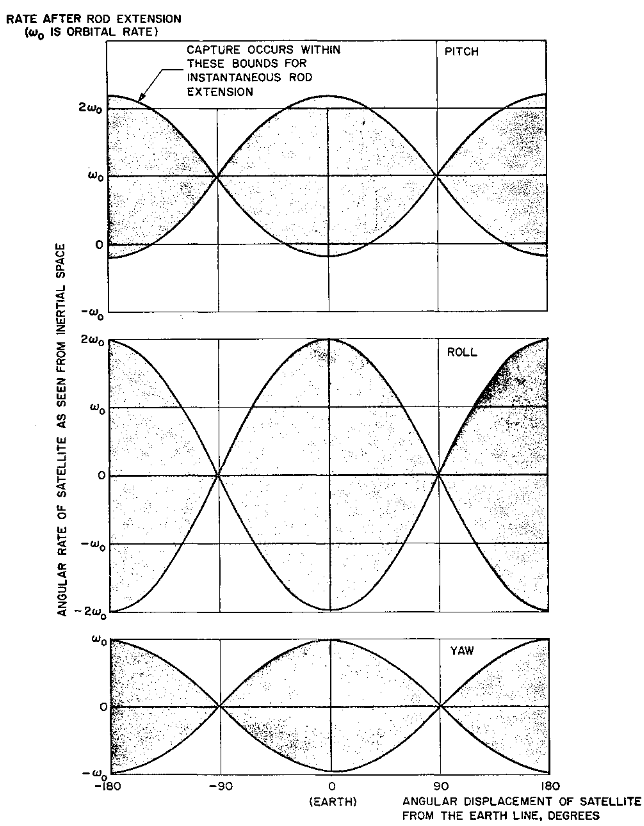

Fig. 1

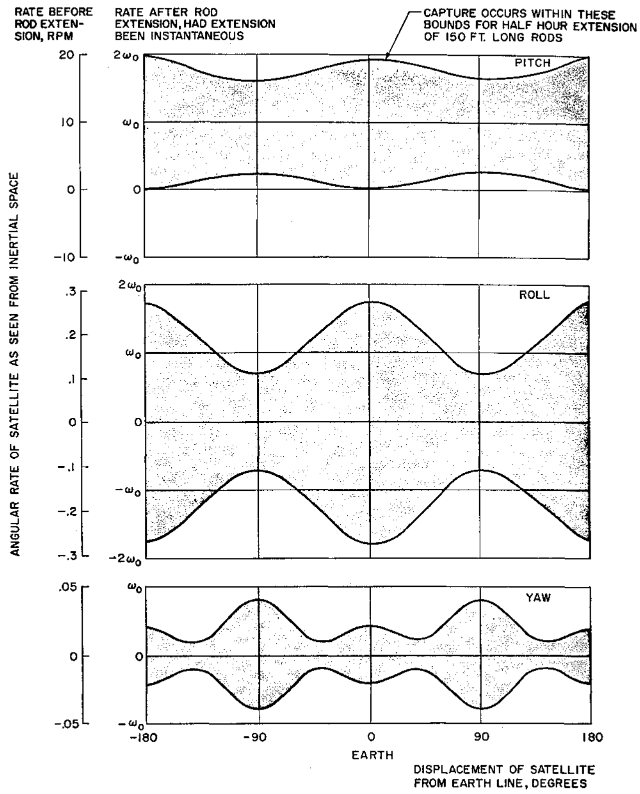

Fig. 2

Three-Axis Motion: Cross Coupling

The foregoing considerations of instantaneous and slow tube extension were planar, one axis taken at a time. In considering three-axis motion, the realistic simultaneous motion of pitch, roll, and yaw cross coupling among the three axes occurs. Before examining capture in three axes, it is well to note the extent of cross coupling for a gravity gradient stabilized satellite. By cross coupling is meant the influence of motions about one axis upon motions about the other two axes. This interaction of the axes is described by Euler's equations, which relate the torques applied to each axis and the resultant rates and accelerations, for a given set of inertias about the three axes. Here the torques are due to the gravity gradient field, the rates are to be found, and the inertias are due to the tubes. Figure 3 (top) shows the extent of cross coupling as it affects the yaw axis typically, after the tubes have been completely extended and the satellite is in orbit rotating about its axis normal to the orbital plane (the pitch axis) at orbital rate. Were there no cross coupling, the motion about the yaw axis, as well as the other two axes, would instead be purely sinusoidal. Figure 3 (top) represents the following case: The orbital altitude is 5000 naut miles. The satellite consists of a central payload from which extend four tubes. Each of the four tubes is 150 ft long, and each weighs $2\frac{1}{4}$ lb. Initially, the satellite has no rate with respect to the earth and is displaced 45° in pitch, roll, and yaw.

Three-Axis Motion: Capture

"Capture" in three-axis motion is defined to mean that the satellite's yaw axis does not exceed a displacement of 90° from the earth line. If captured, motion of the yaw axis stays within one of two "cones," each of 90° half angle. One cone points to earth and the other cone away from earth. Capture in three axes is not a yes or no phenomenon as it was

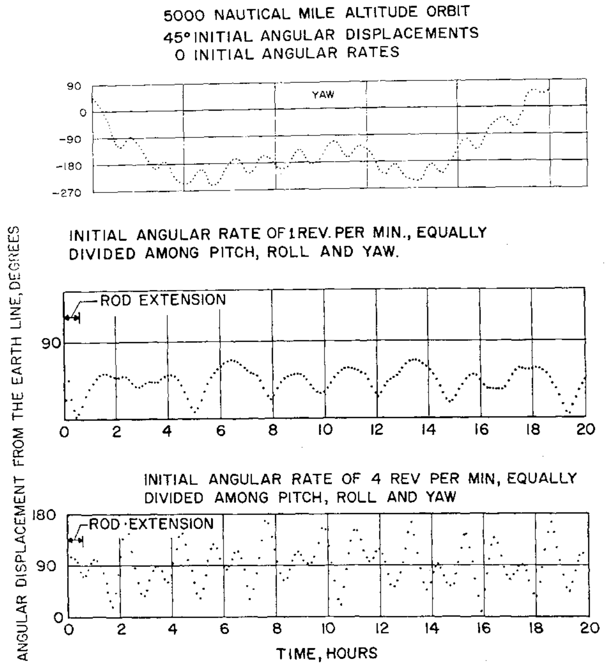

Fig. 3

for planar theory. If the initial tumbling rate is very high, the satellite will indeed tumble after rod extension. For lower initial tumbling rates, the satellite may capture for a while, then tumble, capture again, etc. It is best to examine capture in the light of the initial tumbling that the satellite may be expected to have.

The satellite will be injected into orbit either from a spin-stabilized final propulsion stage or from one having its own attitude stabilization. If the final propulsion stage is spin-stabilized, the satellite is despun by discharging gas or releasing yo-yo weights before extending the tubes. Before extending the tubes, such a satellite will be tumbling about any axis with a rate of 1 rpm typically. Most of this tumbling rate orginally came from misalignment of the thrust vector during spin-up, with the rest coming from the separation mechanism.

If the final propulsion stage has its own attitude stabilization, the satellite before extending its tubes will be tumbling about any axis with a rate of 0.1 rpm typically.

The satellite's motions for an initial rate of 1 rpm are shown in Fig. 3 (middle). At time 0 the tubes are released. At time $\frac{1}{2}$ hr, the tubes are fully extended 150 ft, measured outward from the central payload. The motion is shown by giving the earth pointing error, the angle between the satellite's yaw axis and the local vertical. The initial rate is referenced to inertial space. For Fig. 3 (middle) the initial rate is evenly divided among pitch, roll, and yaw, and the pitch rate is "positive." A positive pitch rate as seen from inertial space is in the same direction as that of the satellite orbiting the earth. The direction of the pitch rate is important for determining whether the satellite captures without damping. It is also important for determining whether it captures with damping, for certain types of damping.

For Fig. 3 (middle) the satellite is captured, since the angle the yaw axis makes with local vertical remains less than 90°. If the 1-rpm initial rate has a negative rather than positive pitch component, it also is captured.

By raising the total rate to 4 rpm with equal components in pitch, roll, and yaw, and a negative pitch rate, the satellite is no longer captured, as seen in Fig. 3 (top). Thus, for initial tumbling rates to be anticipated (up to 1 rpm), the satellite has a good chance of capture at an orbital altitude of 5000 naut miles.

It is sufficient to use the phrase "good chance" of capture. There is no justification for precisely defining the bounds of the capture map until damping is accounted for. All passively stabilized satellites must have some form of damping. Damping will superimpose on the basic capture phenomenon discussed, an added effect converting the initial tumbling to some other motion. The effect depends on the particular damping technique employed, and it is only when the technique has been specified that a precise capture map has mission significance.

Effect of Nose Bluntness on the Flow around a Typical Ballistic Shape

Donald W. Eastman* and Leonard P. Radtke†
The Boeing Company, Seattle, Wash.

THE purpose of this note is to show the effects of nose bluntness on the flow around a typical ballistic shape. Theoretical and experimental results are presented.

Four blunt cone-cylinder-flare combinations tested at $M = 6.10$[1] are shown in Figs. 1–4. The bodies are identical except for the amount of hemispherical nose bluntness. The pressure coefficients measured along the surface of the bodies and the shock shapes obtained from schlieren photographs also are shown. The total temperature and pressure during the test were 550°F and 900 psia, respectively.

A method of characteristics program[2] was used to calculate the flow fields around these bodies. This program has the capability to calculate and cross shock waves caused by flares or flow recompression. Without the capability to calculate recompression shocks, the program would "blow up" at the start of the shock. This type of calculation is probably the most difficult of any connected with the calculation of flow around axisymmetric bodies. Because of the low total temperature of the experiments, an ideal gas with $\gamma = 1.4$ was used for all calculations. The subsonic nose region was calculated using an inverse method program.

Figures 1–4 show a comparison of experimental and theoretical results. Except for the flare region there is an excellent comparison between the two.

Figure 2 illustrates an interesting phenomenon associated with flow around blunt cones. That is, the shock wave caused by the recompression of the flow along the nose cone. If the cone were very long, the pressure eventually would reach the sharp cone value. Since this value is higher than the pressure aft of the blunt nose, the flow must recompress. Thus, the recompression shock is formed. This shock could not be seen in the schlieren photographs. Its effect on the bow shock can be seen, however, by examining Fig. 2 carefully. When the recompression shock intersects the bow shock, the bow shock wave angle increases approximately 1.5°.

Referring to Figs. 1–4, it can be seen that the pressure distribution along the flare definitely is influenced by the amount of nose bluntness. In fact the flare pressures for the sharp body are about twice the values of the completely blunt body. Figures 2–4 show how the high entropy layer from the blunt nose reduces the pressure near the flare juncture. For the slightly blunted body (Fig. 2) the layer is thin, and the pressure distribution aft of the juncture starts to increase to the sharp nose value of Fig. 1. Bluntness effects dominate the flow over the flare in Figs. 3 and 4. However, the

Received June 24, 1963.

* Research Engineer, Aero-Space Division, Flight Technology Department. Member AIAA.

† Research Engineer, Aero-Space Division, Applied Mathematics Organization. Member AIAA.